http://dx.doi.org/10.5012/bkcs.2012.33.4.1235

Effects of Al Concentration on Structural and Optical Properties of Al-doped ZnO Thin Films

Min Su Kim, Kwang Gug Yim, Jeong-Sik Son,† and Jae-Young Leem*

Department of Nano Systems Engineering, Center for Nano Manufacturing, Inje University, Gimhae, Gyungnam 621-749, Korea
**E-mail: jyleem@inje.ac.kr*
†Department of Visual Optics, Kyungwoon University, Gumi, Gyongsanbuk-do 730-850, Korea
Received October 24, 2011, Accepted January 9, 2012

Aluminium (Al)-doped zinc oxide (AZO) thin films with different Al concentrations were prepared by the sol-gel spin-coating method. Optical parameters such as the optical band gap, absorption coefficient, refractive index, dispersion parameter, and optical conductivity were studied in order to investigate the effects of the Al concentration on the optical properties of AZO thin films. The dispersion energy, single-oscillator energy, average oscillator wavelength, average oscillator strength, and refractive index at infinite wavelength of the AZO thin films were found to be affected by Al incorporation. The optical conductivity of the AZO thin films also increases with increasing photon energy.

Key Words : Zinc oxide, Aluminum, Thin film, Sol-gel, Optical parameter

Introduction

Zinc oxide (ZnO) is a direct band gap semiconductor with a band gap of 3.37 eV and large exciton binding energy of 60 meV.[1,2] ZnO thin films have attracted considerable interest in recent years for application as a transparent conducting material in liquid crystal displays,[3] solar cells,[4] *etc*. The conventional transparent conductive oxide (TCO) material is indium tin oxide (ITO). However, ITO materials are very expensive and low stability to H_2 plasma and toxicity. Undoped and doped ZnO thin films are widely used in transparent conducting layers because of their thermal stability and better resistance against hydrogen plasma processing damage compared to ITO.[5,6]

Various techniques such as molecular beam epitaxy (MBE),[7] pulse laser deposition (PLD),[8] magnetron sputtering,[9] chemical vapor deposition (CVD),[10] atomic layer deposition,[11] electron beam evaporation,[12] hydrothermal method,[13] and sol-gel process[14] have been applied to ZnO thin film preparation. The sol-gel method has distinct potential advantages over these other techniques owing to its lower crystallization temperature, low cost, simple deposition procedure, easier compositional control, ability to tune the microstructure *via* sol-gel chemistry, and large surface area coating capability.

As-prepared ZnO usually exhibits *n*-type conductivity, which may be caused by intrinsic defects such as interstitial zinc and oxygen vacancies. The conductivity can be enhanced by introducing elements such as B, Al, Ga, and In. Al-doped ZnO (AZO) thin films exhibit high transparency and low resistivity.[15] However, there have been few reports detailing the optical properties of AZO thin films.

In this work, undoped ZnO and AZO thin films were prepared by the sol-gel method with different Al concentrations. The structural and optical properties of the AZO thin films were investigated. In particular, optical parameters such as the optical band gap, absorption coefficient, Urbach energy, refractive index, dispersion parameter, and optical conductivity were comprehensively studied in order to investigate the effects of Al doping on the optical properties of AZO thin films.

Experimental Details

AZO thin films were deposited on quartz substrates by the sol-gel spin-coating method. Zinc acetate dihydrate [$Zn(CH_3COO)_2{\cdot}2H_2O$] was used as a starting material. Monoethanolamine [C_2H_7NO] and 2-methoxyethanol [$CH_3OCH_2CH_2OH$] were used as the stabilizer and solvent, respectively. The dopant source was aluminum nitrate [$Al(NO_3)_2{\cdot}9H_2O$]. The zinc acetate dihydrate and aluminum nitrate were dissolved in a mixture of 2-methoxyethanol and monoethanolamine (MEA). The molar ratio of dopant in the starting solution was varied to give a [Al/Zn] ratio of 1-3 at.%. The molar ratio of MEA to zinc acetate was maintained at 1.0 and the concentration of zinc acetate was 0.6 M. The resultant solution was stirred at 60 °C for 2 h to yield a clear and homogeneous solution. Finally, the solution was aged at room temperature for 24 h. Prior to deposition, the quartz substrates were carefully cleaned with distilled water, acetone, and ethanol in sequence under ultrasonic irradiation; they were then rinsed with distilled water and lastly dried with N_2 (99.9999%) gas. The solution was dropped on quartz substrates, which were rotated at 3000 rpm for 20 s. The AZO thin films were heated at 300 °C for 10 min to evaporate the solvent and remove the organic residuals (named as pre-heat treatment). After the pre-heat treatment, the AZO thin films were cooled at a cooling rate of 5 °C/min to avoid cracks. The spin-coating and pre-heating processes were repeated five times. For crystalli-

zation, the AZO thin films were heated in a furnace in air atmosphere at 550 °C for 60 min (named as post-heat treatment). The thicknesses of the AZO thin films were about 250 nm for 0 at.%, 230 nm for 1 at.%, 225 nm for 2 at.%, and 220 nm for 3 at.%. The microstructure was investigated by using a scanning electron microscope (SEM). The crystallinity and orientation of the AZO thin films were measured by X-ray diffraction (XRD). The optical transmittance and reflectance of the AZO thin films were measured as a function of wavelength by UV-visible spectroscopy.

Results and Discussion

Surface Morphological and Structural Properties of the AZO Thin Films. Figure 1 shows SEM images of the AZO thin films with different Al concentrations: (a) 0, (b) 1, (c) 2, and (d) 3 at.%. All the thin films exhibited a rough surface with three-dimensional (3D) island growth due to the lattice and chemical mismatches between the thin films and substrates. These factors made the surface of the thin films rough. The particle size was significantly reduced by Al incorporation into the AZO thin films.

Figure 2 shows XRD spectra of the AZO thin films with different Al concentrations: (a) 0, (b) 1, (c) 2, and (d) 3 at.%. The diffraction peaks of undoped ZnO and AZO thin films indicate the hexagonal wurtzite structure of the thin films.[16] Figure 3 shows the full width at half maximum (FWHM) of the ZnO (002) diffraction peak and average grain size of the AZO thin films as a function of the Al concentration. The FWHM increased from 0.16° to 0.32° as the Al concentrations were increased. The FWHM was closely related to the grain size of the thin films. The average grain size was determined using Scherrer's equation[17]:

$$D = \frac{0.9\lambda}{\beta\cos\theta} \quad (1)$$

where λ is the X-ray wavelength, θ is the Bragg angle of the ZnO (002) diffraction peak, and β is the FWHM in radians. The average grain size decreased from 60 to 30 nm when the Al concentration was increased from 0 to 3 at.%. The AZO thin films exhibited a smaller grain size than the undoped ZnO thin films; this can be attributed to the increase in Al.[18] These results were in good agreement with the SEM images. For Al doping, the concentration of the zinc interstitials was reduced for charge compensation; this resulted in suppressed ZnO grain growth and deteriorated crystallinity.[19]

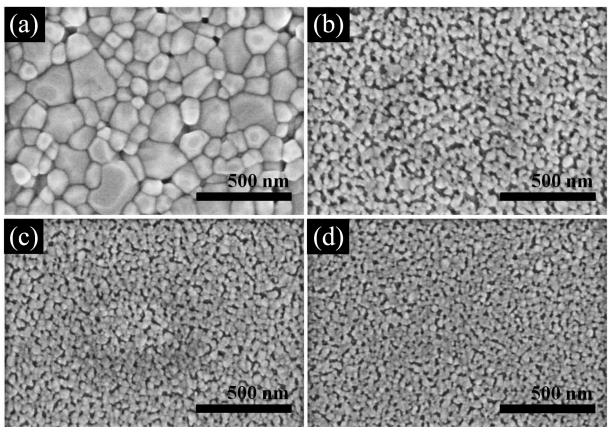

Figure 1. SEM images of the AZO thin films with different Al concentration: (a) 0, (b) 1, (c) 2, and (d) 3 at.%.

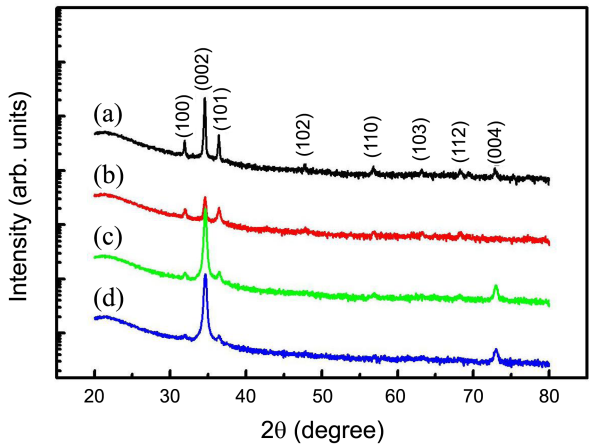

Figure 2. XRD spectra of the AZO thin films with different Al concentration: (a) 0, (b) 1, (c) 2, and (d) 3 at.%.

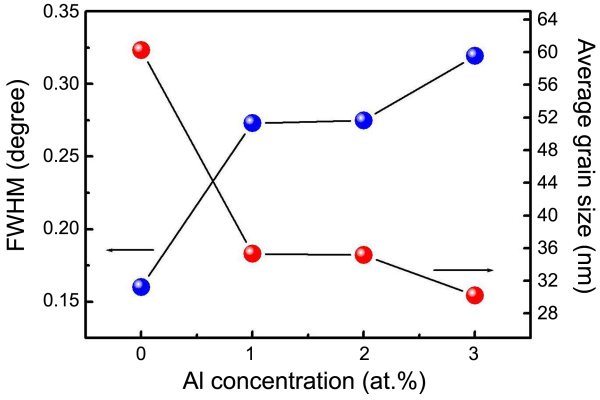

Figure 3. FWHM of the ZnO (002) diffraction peak and the average grain size of the AZO thin films as a function of the Al concentration.

Figure 4 shows the residual stress and bond length in the AZO thin films as a function of the Al concentration. The residual stress (σ) in the AZO thin films can be expressed as[20]

$$\sigma = \frac{2C_{13}^2 - C_{33}(C_{11}+C_{12})}{2C_{13}} \times \frac{c-c_0}{c_0} \quad (2)$$

where C_{ij} are elastic stiffness constants for ZnO (C_{11} = 207.0 GPa, C_{33} = 209.5 GPa, C_{12} = 117.7 GPa, and C_{13} = 106.1 GPa). c and c_0 are the lattice constants of the AZO thin films and strain-free ZnO thin films, respectively. If the stress is positive, the biaxial stress is tensile; if the residual stress is negative, the biaxial stress is compressive. The residual stress of the undoped ZnO thin films was smaller than that of the AZO thin films. The residual stress of the AZO thin films increased as the Al concentration was increased to 2 at.%. There seems to be a critical value for the Al

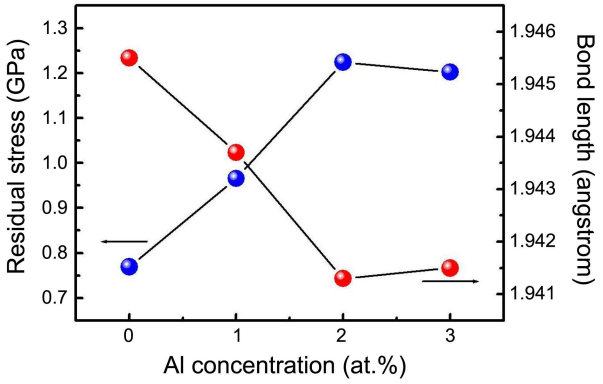

Figure 4. Residual stress and bond length of Zn-O in the AZO thin films as a function of the Al concentration.

concentration in AZO up to which stress increases and after which it decreases. Above this critical value, the Al atoms, rather than substituting at the Zn sites, may go to the interstitial sites; the *c* lattice parameter showed an increase compared with the AZO thin films with Al concentration of 1 and 3 at.%. The total residual stress in the thin films mainly consisted of two components: the intrinsic stress introduced by the doping and defects during the growth, and the extrinsic stress introduced by the mismatch in lattice constants and thermal expansion coefficients of the thin films and substrates. In the case of the AZO thin films, the pre- and post-heat treatments were kept the same for all of the thin films; therefore the intrinsic stress originating from the thermal mismatch between the thin films and substrates was expected to be of the same magnitude for all of the thin films. Thus, the observed change in the residual stress of the AZO thin films was mainly from the doping of Al and changes in the defects of the ZnO thin films resulting from the change in the bond length (*L*) of Zn-O in the AZO thin films. The bond length of the AZO thin films is given by[21]

$$L = \sqrt{\left(\frac{a^2}{3} + \left(\frac{1}{2} - u\right)^2 c^2\right)} \tag{3}$$

where *u* is given by (in the wurtzite structure)

$$u = \frac{a^2}{3c^2} + 0.25 \tag{4}$$

and is related to the *a*/*c* ratio. The bond length decreased as the Al concentration was increased to 2 at.%, which was the inverse trend in comparison with the residual stress.

Absorption Coefficient and Optical Band Gap of the AZO Thin Films. Figure 5 shows the optical transmittance of the AZO thin films with different Al concentrations. The optical transmittance clearly exhibited a shift in band edge due to the variation in Al concentrations with a transparency of 80% in the visible range (400-700 nm). The optical transmittance of the ZnO thin films is known to be determined by the thickness, surface roughness, and absorption coefficient of the thin films. The absorption coefficient $\alpha(\lambda)$ of the ZnO-based materials can simply be calculated by[22]

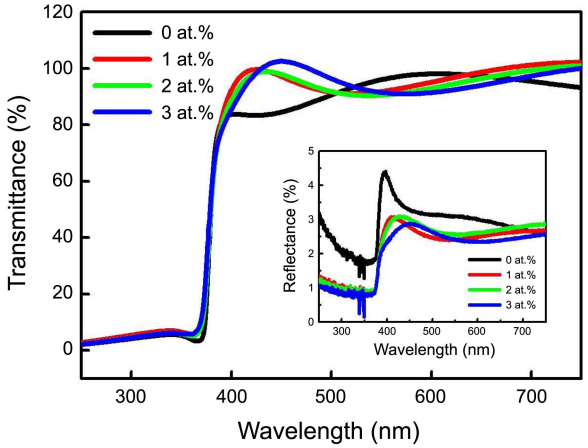

Figure 5. Optical transmittance of the AZO thin films with different Al concentrations. The inset shows the reflectance of the AZO thin films.

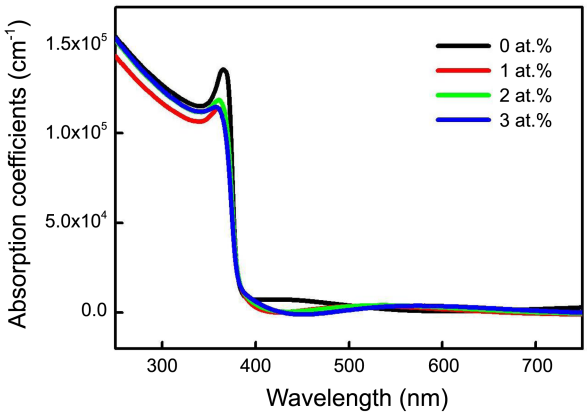

Figure 6. Absorption coefficient of the AZO thin films with different Al concentrations.

$$T = \exp[-\alpha(\lambda)d] \tag{5}$$

where *T* is the optical transmittance, $\alpha(\lambda)$ is the absorption coefficient, and *d* is the thickness of the thin films. The inset shows the reflectance of the AZO thin films. The reflectance decreased with Al incorporation, which was due to the increase in the voids of the AZO thin films.

The absorption coefficient can be obtained through $I = I_0 e^{-\alpha t}$, where *I* and I_0 are the intensities of the transmitted and incident light, respectively, and *t* is the thickness of the AZO thin films. Figure 6 shows the absorption coefficient (α) of the AZO thin films with different Al concentrations. In the direct transition semiconductor, the absorption coefficient (α) follows the following relationship optical band gap (E_g)[23]

$$\alpha h\nu = B(h\nu - E_g)^{1/2} \tag{6}$$

where *h* is Planck's constant, *v* is the frequency of the incident photon, and *B* is a constant that depends on the electron-hole mobility. In addition, the absorption coefficient is in the range of 10^4 to 10^5 cm^{-1} when $h\nu > E_g$.[24] The absorption coefficients in the UV region were larger than

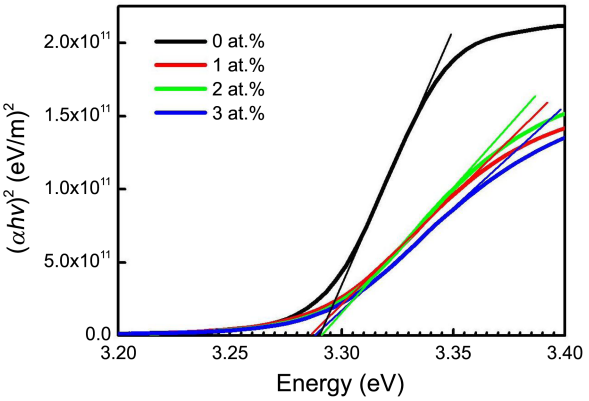

Figure 7. Plots of $(\alpha hv)^2$ *vs*. photon energy of the AZO thin films with different Al concentrations.

those in the visible region and decreased with Al incorporation. Nevertheless, those in the UV region changed little with Al incorporation, which may be due to the decrease in the optical band gap. These results imply that the optical absorption in the UV region of the AZO thin films can be decreased by Al incorporation and the absorption coefficient is a wave-number-dependent function.

The optical band gap can be determined by extrapolation of the linear region from the α^2 *vs*. $h\nu$ plot near the onset of the absorption edge to the energy axis. Figure 7 shows the plots of $(\alpha hv)^2$ *vs*. photon energy of AZO thin films with different Al concentrations. The optical band gap of the undoped ZnO thin films was found to be about 3.291 eV. The optical band gap of the AZO thin films slightly decreased with Al incorporation, which agrees with the literature.[25] Generally, the literature has shown that the optical band gap of the AZO films increases with increasing Al doping concentration.[26] However, our experiment showed the opposite effect, which may be attributed to the band shrinkage effect because of increasing carrier concentration.[27]

Refractive Index and Dielectric Constants of the AZO Thin Films. The refractive index is an important parameter for optical materials and applications. Thus, it is important to determine optical constants of the thin films and the complex optical refractive index is described by the following relation[28]:

$$\hat{n} = n(\omega) + ik(\omega) \tag{7}$$

where n is the real part and k is the imaginary part (extinction coefficient) of the complex refractive index. The refractive index of the films was determined from the following relation[29]:

$$n = \left(\frac{1+R}{1-R}\right) + \sqrt{\frac{4R}{(1-R)^2} - k^2} \tag{8}$$

where k ($k = \alpha\lambda/4\pi$) is the extinction coefficient. The extinction coefficient can be calculated from the optical transmittance. Figure 8 shows the (a) refractive index (n) and (b) extinction coefficient (k) of the AZO thin films with different Al concentrations. The refractive index and extinction coefficient of the AZO thin films decreased with Al incorporation. The decrease in the refractive index with Al incorporation was mainly attributed to an increase in the carrier concentration in the AZO thin films. For all of the AZO thin films, the refractive index in visible region changed only slightly and tended to be a constant at ~1.4, which is in good agreement with the results calculated by Bandyopadhyay *et al*..[30]

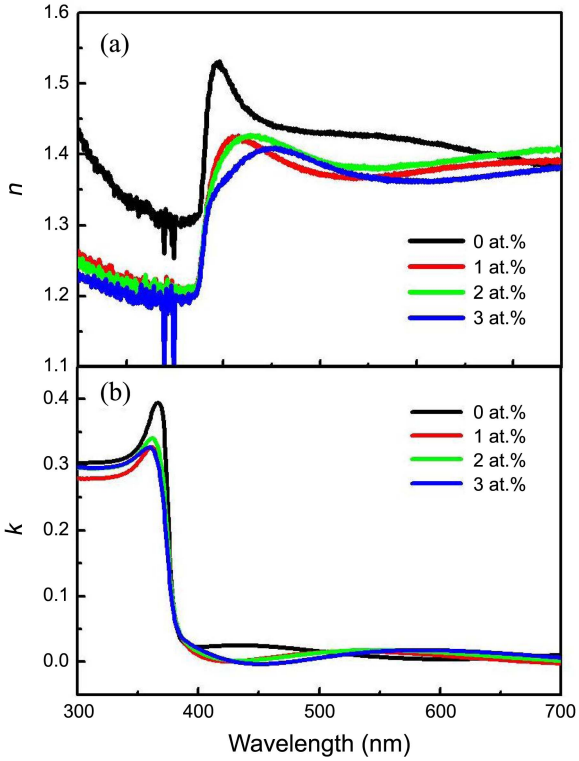

Figure 8. (a) Refractive index and (b) extinction coefficient of the AZO thin films with different Al concentrations.

The refractive index dispersion plays an important role in optical communication and the design of optical devices. Thus, it is important to determine the dispersion parameters of the films. The dispersion parameters of the films were determined from the relation given by[31]

$$n^2 - 1 = \frac{E_o E_d}{E_o^2 - E^2} \tag{9}$$

where E_o is the single-oscillator energy and E_d is the dispersion energy, which is a measure of the intensity of the inter band optical transitions. Figure 9 shows the plots of $(n^2-1)^{-1}$ *vs*. $(h\nu)^2$ of the AZO thin films with different Al concentrations. The E_o and E_d values were determined from the slope $(E_o E_d)^{-1}$ and intercept (E_o/E_d) on the vertical axis and are given in Table 1. The values of the single-oscillator and dispersion energy increased with increasing Al concentration. The increase in dispersion energy is usually associated with the evolution of the AZO thin films microstructure to a more ordered phase.[32]

The dispersion data of refractive index was also fitted by the following relation:

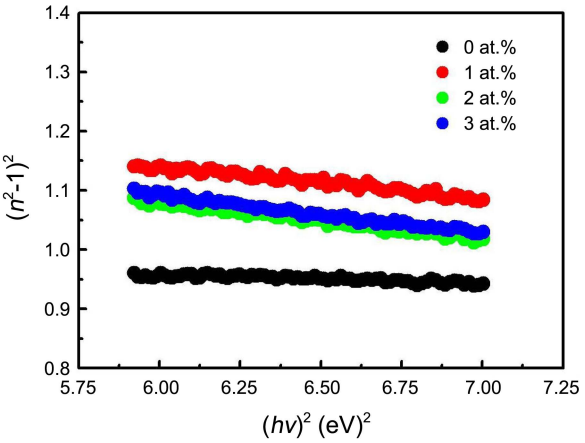

Figure 9. Plots of $(n^2-1)^{-1}$ *vs.* $(h\nu)^2$ of the AZO thin films with different Al concentrations.

$$n^2-1=\frac{S_o\lambda_o^2}{1-(\lambda_o/\lambda)^2} \tag{10}$$

where λ is the wavelength of incident light, S_o is the average oscillator strength and λ_o is an average oscillator wavelength. The S_o and λ_o values were obtained from the slope $(1/S_o)$ and intercept $(S_o\lambda_o)^{-1}$ of the plotted curves and are given in Table 1. When the Al concentrations were increased, the value of the average oscillator strength decreased, while the value of the average oscillator wavelength increased.

The refractive index at infinite wavelength (n_∞) can be obtained from the relation

$$\frac{n_\infty^2-1}{n^2-1}=1-\left(\frac{\lambda_o}{\lambda}\right)^2 \tag{11}$$

The plots of $(n^2-1)^{-1}$ *versus* λ^{-2} were plotted to obtain the n_∞ values. The values of the refractive index at infinite wavelength changed with increasing Al concentration.

The fundamental electron excitation spectrum of the films was described by means of the frequency dependence of the complex dielectric constant. The real (ε_1) and imaginary (ε_2) parts of the dielectric constant are related to the n and k values. The ε_1 and ε_2 values were calculated using the following formulas[33]:

$$\varepsilon_1=n^2-k^2 \tag{12}$$

$$\varepsilon_2=2nk \tag{13}$$

The dependence of ε_1 and ε_2 on photon energy is respectively shown in Figures 10(a) and (b). The ε_1 and ε_2 values sharply changed in the visible region. The value of ε_2 of the AZO thin films was lower than that of the undoped ZnO thin films, which indicates low dielectric loss in the AZO thin films.

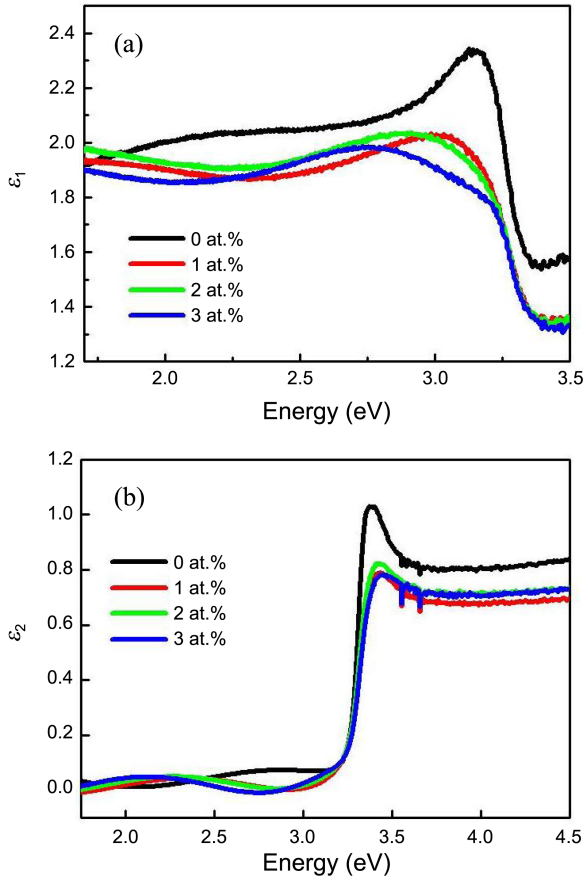

Figure 10. Variation in (a) real and (b) imaginary parts of the dielectric constant of the AZO thin films with different Al concentrations.

***M*$_{-1}$ and *M*$_{-3}$ Moments of the Optical Spectra from the AZO Thin Films.** The single-oscillator parameters E_o and E_d are related to the imaginary component ε_i of the complex dielectric constant. The ε_i parameter includes the desired response information about the electronic and optical properties of the optical material. Thus, determining the moments of the ε_i spectrum is very important for developing optical applications of the optical material under study. The M_{-1} and M_{-3} moments of the optical spectra can be obtained from the following relations

Table 1. Optical parameters such as the optical band gap, dispersion energy, single-oscillator energy, average oscillator wavelength, M_{-1} and M_{-3} moments, average oscillator strength, and refractive index at infinite wavelength of the AZO thin films with different Al concentrations

Al concentrations	E_g (eV)	E_d (eV)	E_o (eV)	λ_o (nm)	M_{-1}	M_{-3} (eV)$^{-2}$	S_o (10^{13} m^{-2})	n_∞
0 at.%	3.291	0.126	0.134	146.69	0.017	1.059	5.44	1.473
1 at.%	3.287	0.191	0.277	287.98	0.053	1.455	1.52	1.505
2 at.%	3.293	0.209	0.305	368.71	0.064	1.459	1.23	1.636
3 at.%	3.289	0.214	0.322	419.81	0.069	1.507	0.97	1.643

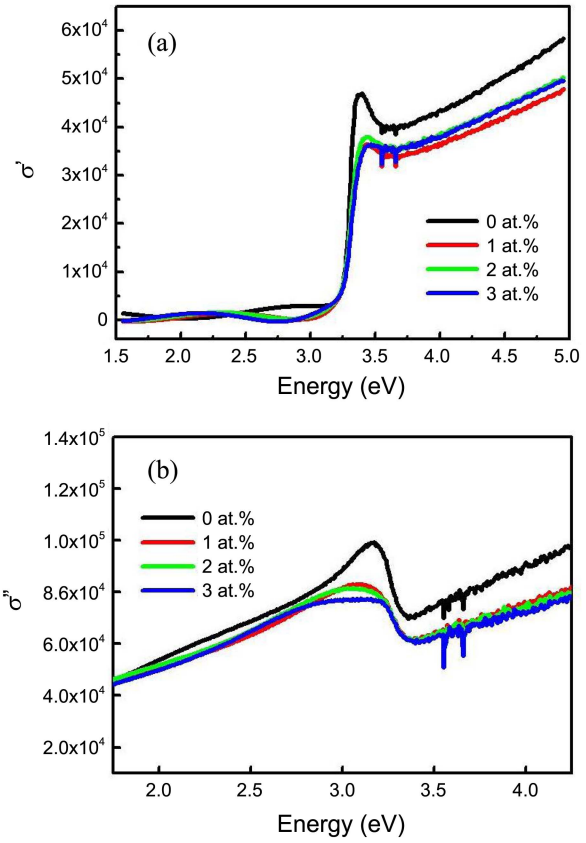

Figure 11. Variation in (a) real and (b) imaginary parts of the optical conductivity of the AZO thin films with different Al concentrations.

$$E_o^2 = \frac{M_{-1}}{M_{-3}} \quad (14)$$

$$E_d^2 = \frac{M_{-1}^3}{M_{-3}} \quad (15)$$

The obtained values are given in Table 1. The obtained M_{-1} and M_{-3} moments increased with the Al concentrations.

Optical Conductivity Properties of the AZO Thin Films. The real σ' and imaginary σ'' parts of the optical conductivity are described as[33]

$$\sigma' = \omega\varepsilon_2\varepsilon_0 \quad (16)$$

$$\sigma'' = \omega\varepsilon_1\varepsilon_0 \quad (17)$$

where ω is the angular frequency and ε_0 is the free space dielectric constant. The real and imaginary parts of the optical conductivity dependence of energy are shown in Figures 11(a) and (b), respectively. Both of the σ' and σ'' values were also affected by the Al incorporation. σ' of the AZO thin films was low for low values of energy and drastically increased with energy corresponding to the band gap energy, which may be due to electrons excited by photon energy. σ' decreased at higher energies than the optical band gap with Al incorporation. This may be because the absorption coefficient of the AZO thin films decreased with Al incorporation as shown in Figure 6.

Conclusions

AZO thin films were prepared with different Al concentrations by the sol-gel spin-coating method and their optical parameters at wavelengths of 250-750 nm were investigated. The optical band gap of the AZO thin films was not significantly affected by Al incorporation. However, the dispersion energy, single-oscillator energy, average oscillator wavelength, average oscillator strength, and refractive index at infinite wavelength of the AZO thin films were affected by Al incorporation. In addition, the optical conductivity of the AZO thin films increased with increasing energy.

Acknowledgments. This work was supported by the 2012 Inje University research grant.

References

1. Hümmer, K. *Phys. Status Solidi B* **1943**, *56*, 249.
2. Wong, E. M.; Searson, P. C. *Appl. Phys. Lett.* **1999**, *74*, 2939.
3. Oh, B.-Y.; Jeong, M.-C.; Moon, T.-H.; Lee, M. W.; Myoung, J.-M. *J. Appl. Phys.* **2006**, *99*, 124505.
4. Keis, K.; Magnusson, E.; Lindström, H.; Lindquist, S.-E.; Hagfeldt, A. *Sol. Energy Mater. Sol. Cells* **2002**, *73*, 51.
5. Song, Y.; Kim, E. S.; Kapila, A. *J. Electron. Mater.* **1995**, *24*, 83.
6. Ip, K.; Overberg, M. E.; Heo, Y. W.; Norton, D. P.; Pearton, S. J.; Kucheyev, S. O.; Jagadish, C.; Wiliams, J. S.; Wilson, R. G.; Zavada, J. M. *Appl. Phys. Lett.* **2002**, *81*, 3996.
7. Yim, K. G.; Cho, M. Y.; Jeon, S. M.; Kim, M. S.; Leem, J.-Y. *J. Korean Phys. Soc.* **2011**, *58*, 520.
8. Kaidashev, E. M.; Lorenz, M.; Wenckstern, H.; Rahm, A.; Semmelhack, H.-C.; Han, K.-H.; Benndorf, G.; Bundesmann, C.; Hochmuth, H.; Grundmann, M. *Appl. Phys. Lett.* **2003**, *82*, 3901.
9. Carcia, P. F.; Mclean, R. S.; Reilly, M. H.; Nunes, G. *Appl. Phys. Lett.* **2003**, *82*, 1117.
10. Gorla, C. R.; Emanetoglu, N. W.; Liang, S.; Mayo, W. E.; Lu, Y.; Wraback, M.; Shen, H. *J. Appl. Phys.* **1999**, *85*, 2595.
11. Kim, Y.-S.; An, C. J.; Kim, S. K.; Song, J.; Hwang, C. S. *Bull. Korean Chem. Soc.* **2010**, *31*, 2503.
12. Kuroyanagi, A. *Jpn. J. Appl. Phys.* **1989**, *28*, 219.
13. Kim, M. S.; Yim, K. G.; Jeon, S. M.; Lee, D.-Y.; Kim, J. S.; Kim, J. S.; Son, J.-S.; Leem, J.-Y. *Jpn. J. Appl. Phys.* **2011**, *50*, 035003.
14. Kim, M. S.; Yim, K. G.; Leem, J.-Y.; Kim, S.; Nam, G.; Kim, D. Y.; Kim, S.-O.; Lee, D.-Y.; Kim, J. S.; Kim, J. S. *J. Korean Phys. Soc.* **2011**, *59*, 346.
15. Agura, H.; Suzuki, A.; Matsushita, T.; Aoki, T.; Okuda, M. *Thin Solid Films* **2003**, *445*, 263.
16. Berber, M.; Bulto, V.; Kliß, R.; Hahn, H. *Scripta Mater.* **2005**, *53*, 547.
17. Williamson, G. B.; Smallman, R. C. *Philos. Mag.* **1956**, *1*, 34.
18. Gupta, B.; Jain, A.; Mehra, R. M. *J. Mater. Sci. Technol.* **2010**, *26*(3), 223.
19. Fujihara, S.; Suzuki, A.; Kimura, T. *J. Appl. Phys.* **2003**, *94*, 2411.
20. Hong, R. J.; Huang, J. B.; He, H. B.; Fan, Z. X.; Shao, J. D. *Appl. Surf. Sci.* **2005**, *242*, 346.
21. Barret, C. S.; Massalski, T. B. *Structure of Metals*; Pergamon Press: Oxford, 1980.
22. Kim, K. H.; Park, K. C.; Ma, D. Y. *J. Appl. Phys.* **1997**, *81*, 7764.
23. Jain, A.; Sagar, P.; Mehra, R. M. *Solid State Electron.* **2006**, *50*, 1420.
24. Dragoman, D.; Dragoman, M. *Optical Characterization of Solids*; Springer-Verlag: Heidelberg, 2002.
25. Wang, M.; Lee, K. E.; Hahn, S. H.; Kim, E. J.; Chung, J. S.; Shin, E. W.; Park, C. *Mater. Lett.* **2007**, *61*, 1118.
26. Rozati, S. M.; Akesteh, S. *Mater. Charact.* **2007**, *58*, 319.

27. Minami, T.; Kakumu, T.; Takeda, Y. *Thin Solid Films* **1996**, *290-291*, 1.
28. Yakuphanoglu, F.; Cukurovali, A.; Yilmaz, I. *Opt. Mater.* **2005**, *27*, 1363.
29. Abeles, F. *Optical Properties of Solids*; North-Holland Publishing Company: London, UK, 1972.
30. Bandyopadhyay, S.; Paul, G. K.; Sen, S. K. *Sol. Energy Mater. Sol. C* **2002**, *71*, 103.
31. Shim, H. S.; Han, N. S.; Seo, J. H.; Park, S. M.; Song, J. K. *Bull. Korean Chem. Soc.* **2010**, *31*, 2675.
32. Quasrawi, A. F.; Shukri Ahmad, M. M. *Cryst. Res. Technol.* **2006**, *41*, 364.
33. Hodgson, J. N. *Optical Absorption and Dispersion in Solids*; Chapman and Hall Ltd.: 11 New fetter Lane London EC4, 1970.